Research Article

Computational Design of Next-Generation mTOR Inhibitors that Interfere with Cancer Metabolism

Harish Kumar, M Elizabeth Sobhia*

Department of Pharmacoinformatics
National Institute of Pharmaceutical Education and Research (NIPER),
Sector - 67, S. A. S. Nagar (Mohali),
Punjab - 160062, India
mesophia@niper.ac.in*

Cancer metabolism is one of the hallmarks that cause the alteration in the Metabolic activities in cancer cells as compared to normal body cells. Many different signalling pathways are involved during cancer metabolism, although stimulation of the mTOR-PI3K-AKT pathway is highly anticipated for tumour growth and development. The crucial role of the mTOR complex in major activities, consequentially, excites the researchers to target the complex for therapeutic applications. Reported studies have accounted for the clinical use of mTOR-based inhibitors and many are in the pipeline. Contrastingly, drug resistance and toxicity have considerably limited the use of these inhibitors. Our research is focused on designing next-generation molecules against the target to produce effective therapy that binds to two cavities simultaneously. The workflow follows constructing a pharmacophore map for the early filtering of ligands from expensive computational calculations, followed by molecular docking to find out high-affinity molecules in the protein environment. These high-affinity ligands were utilised for designing next-generation mTOR inhibitors. Common linkers such as Alkyl and PEG were used to tether hits of the allosteric site and kinase site together. Molecule 1 was able to bind in both the cavity with stronger affinity and thus, can be considered as an important hit for inhibiting the mTOR sites. Hence, designed molecules can be clinically tested which may interfere with mTOR activity and can act as a suitable therapy for cancer.

Introduction

Cancer is the second leading cause of death, characterized by uncontrollable cell growth that spreads to surrounding tissues. Cancer cells exhibit multiple characteristics that contribute to the formation of malignant tumours, including uncontrolled growth and division, limitless cell divisions, avoidance of programmed cell death, promotion of blood vessel construction and invasion of tissue to form metastatic tumours.[1,2] Tumour cells require Adenosine Triphosphate (ATP) as a source of energy acquire from catabolism, produce various macromolecules (anabolism) and balance the electrons in the cell i.e., redox balance (Oxidation-reduction). This may lead to alteration in the activity of cells in the tissues or organs which is responsible for the tumour formation leading to cancer. Various metabolic processes occur in cancerous cells dissimilar from those of normal body cells.[3,4] Reprogramming of cellular functioning occurs, leading to various cellular metabolite formation which benefits the growth and proliferation of cells at a higher rate.[5]

The proteins, lipids, and nucleic acids are the three macromolecular classes, most commonly studied in cancer metabolism and constitute approximately 60%, 15%, and 5% of the dry mass of human cells, respectively.[4,6] Biosynthesis of all these is under the control of the same signalling pathways that help in cell growth and are activated in cancer via tumour promoting mutations, particularly Phosphate-Inositol Kinase-3, Protein Kinase, and mammalian Target of Rapamycin (PI3K-AKT-mTOR) signalling pathway. The cellular activities are regulated by the PIK3-AKT-mTOR Complex. This complex is stimulated during cell growth, proliferation, division, and autophagy prevention. Mechanistic target of Rapamycin (mTOR) controls cell growth by promoting anabolic processes like protein, nucleotide, and lipid synthesis, as well as autophagy by breaking down

macromolecules such as glucose and TCA cycle metabolites. mTOR phosphorylates proteins involved in these pathways.[7] Factors like induction of HIF-1, increased ROS concentration, ATP/AMP imbalance, and certain amino acids like glutamine and fumarate activate the PIK3-AKT-mTOR pathway, leading to macromolecule formation and cell division. Mutations in this pathway can result in genetic disorders and increased cancer risk, including Cowden's disease (associated with PTEN functional decrease), tuberous sclerosis complex (mutations in TSC1 or TSC2 genes), and Peutz-Jeghers syndrome (mutation in LKB1 gene).[8]

mTOR plays a critical role in physiology, metabolism, and ageing. Dysregulation of mTOR is associated with diseases like cancer and epilepsy. The mTOR pathway involves proteins activated by growth factor receptors, insulin concentration changes, amino acids, and energy demand. It has garnered attention as a potential anticancer therapy.[9,10] mTOR influences the G1 phase of the cell cycle, delaying it and preventing the S-phase. mTOR exists in two complexes, mTORC1 and mTORC2, which have different subunits and functions. mTORC1 senses nutrients, energy, and redox states, and is primarily involved in protein synthesis. mTORC2 is involved in the actin cytoskeleton and phosphorylation of growth factor receptor-1. DEPTOR, an inhibitory component, can interact with both mTORC1 and mTORC2.[11-13]

PI3K-AKT-mTOR INHIBITORS

The PI3K-AKT-mTOR pathway is commonly activated in the development of cancer cells, and research is focused on inhibiting this pathway. Various molecules have been designed to target different components of the pathway. Some of them inhibit PI3K, such as pan inhibitors like LY294002 and selective inhibitors like ZSTK474.[14] Dual inhibitors like XL765 and BEZ235 target both PI3K and mTOR while clinical trial molecules such as GSK690693 and Perifosine inhibit the activity of AKT protein.[15-17] Rapamycin and its analogues, known as rapalogues, are first-generation mTOR inhibitors.[18] Second-generation mTOR inhibitors, known as ATP-binding site inhibitors or TORKi, target both mTORC1 and mTORC2. Examples include AZD8055 and AZD2014.[19] The third-generation mTOR inhibitor, RapaLink-1, simultaneously binds to the allosteric and kinase site of the mTOR complex. These molecules have been shown to outperform rapamycin or TORKi in both efficacy and

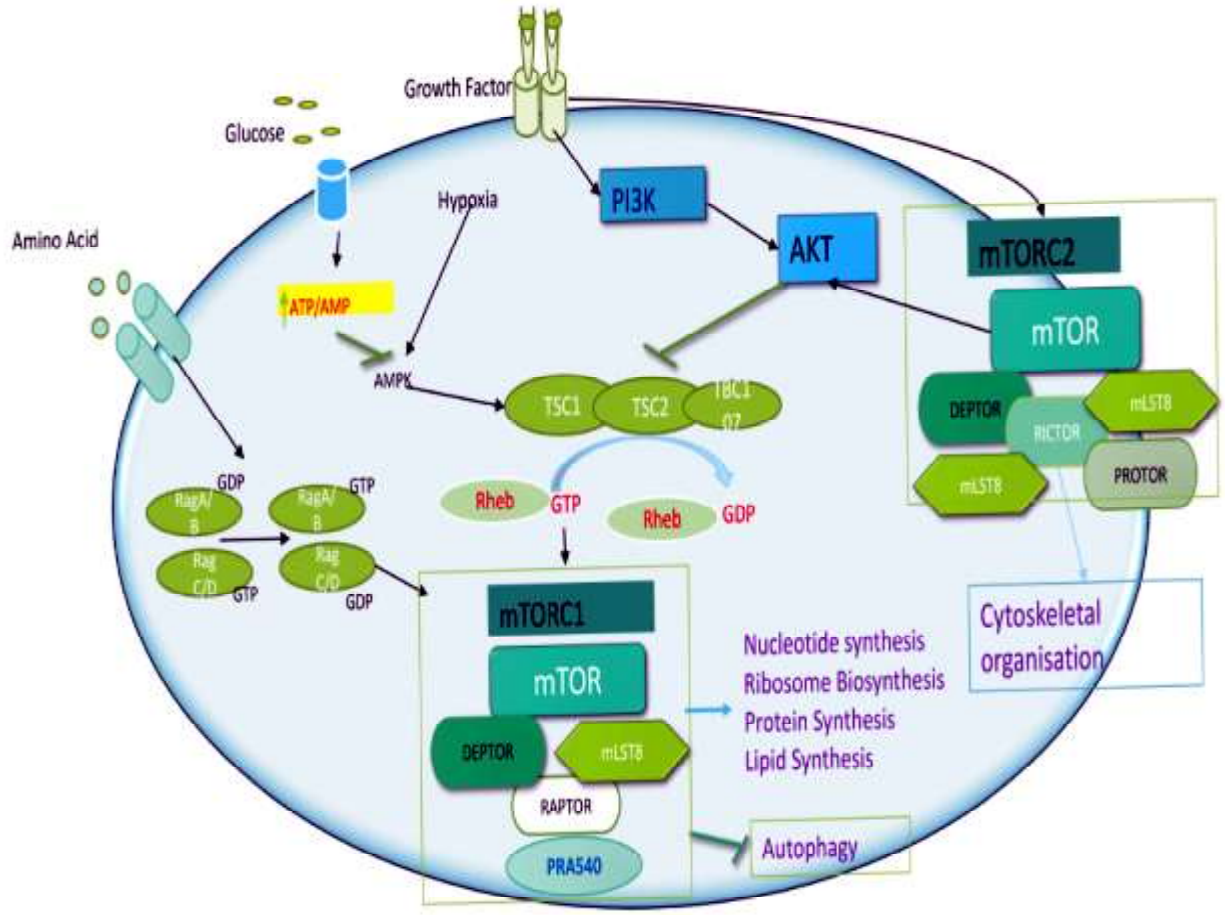

Figure 1. Activation mechanism of PI3K-AKT-mTOR signalling Pathway that is involved in different cellular processes such as nucleotide synthesis, ribosome biosynthesis, protein and lipid synthesis, autophagy etc.

Table 1. Different molecules used in cancer treatment acting via the PI3K-AKT-mTOR pathway

S.N	Molecule	Target	IC50	Patient Population
1.	LY294002	Pan PI3K	0.08 μM	Advanced solid Tumors
2.	Wortmannin	Pan PI3K	16 nM	Advanced solid Tumors
3.	XL765	Selective P13K, mTOR	39 nM (PI3K), 363 nM (mTOR)	Advanced solid Tumors
4.	GSK690693	Pan-AKT	2-14 nM	Advanced solid Tumors
5.	Perifosine	AKT Translocation	9.7 μM	Advanced solid tumor, non-small cell lung cancer, Sarcoma
6.	Rapamycin	mTOR	0.1 to 10 nM	Non-small cell lung cancer (NSCLC), Renal cell carcinoma, Gastrointestinal stromal tumors (GIST)
7.	Temsirolimus	mTOR	1.39 nM	Advanced solid tumours, prostate, breast cancer, chronic lymphocytic leukaemia
8.	AZD2014	TORKIs	2.8 nM	Advanced solid tumours, VEGF-refractory metastatic RCC
9.	AZD8055	TORKIs	0.8 nM	Advanced hepatocellular carcinoma
10.	MLN0128	TORKIs	NA	castration-resistant prostate cancer (CRPC), triple-negative breast cancer (TNBC),
11.	Rapalinks	Both mTOR and TORKIs	NA	Tested in rapamycin-resistant cell lines and mouse xenografts

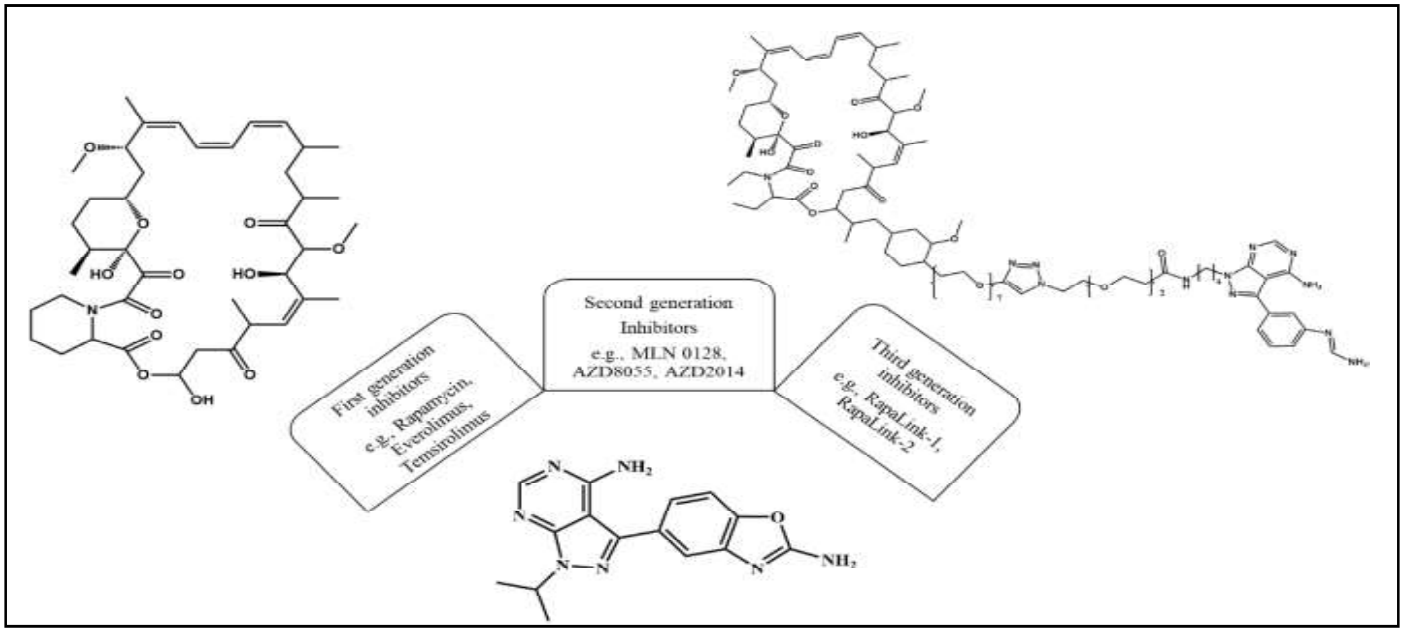

Figure 2. Different types of mTOR inhibitors

lack of drug resistance in animal models. These inhibitors offer the potential for targeted therapy in various types of cancers such as advanced cancer, relapsed and other resistant cancers.[20,21]

The clinical benefit of Rapalogues, such as rapamycin, has been limited due to the insensitivity of certain mTORC1 substrates to their phosphorylation. Negative feedback loops are also activated, promoting cell survival and limiting the efficacy of these inhibitors. Second-generation mTOR kinase inhibitors are undergoing clinical trials but face challenges in gaining approval due to their potential to suppress mTORC1 and activate negative feedback loops, leading to pathway reactivation. Dual inhibitors, although promising, have shown increased toxicity. PI3K and mTOR dual kinase inhibitors like PI-103 offer potential as alternative treatments, but their toxicity levels need to be carefully considered. Additionally, mutations in the gene encoding mTOR have been observed in patients

who did not respond to first- and second-generation inhibitors.[22] Third-generation molecules, which combine rapamycin with TORKi, have shown improved efficacy and binding to resistant cells in animal models while showing reduced toxicity. Third-generation mTOR inhibitors are being developed to address the limitations of earlier versions, focusing on improved selectivity, efficacy, and overcoming resistance. These inhibitors aim to enhance safety, target alternative pathways, enable combination therapies, and achieve precise modulation of mTOR signalling for advanced cancers.[23]

METHODOLOGY

Protein crystal structure selection

In the protein databank (PDB), there was no single structure for mTOR protein which had both the sites (allosteric and kinase site) in one crystal. Therefore, two different crystal structures were obtained from PDB [PDB IDs: 4DRI contains allosteric site & 4JSV contains kinase site].[24,25] 4DRI contained an allosteric site with rapamycin as a co-crystalized ligand. This structure had two chains, peptidyl-prolyl cis-trans isomerase FKBP5 (from residue 20 to 140; chain A) and serine/threonine-protein kinase mTOR (from residue 2017 to 2112; chain B) with a high resolution of 1.45 Å. 4JSV also contained two chains where one chain was serine/threonine-protein kinase mTOR (from residues 1385 to 2549; Chain A) having ATP as co-crystal ligand while the other chain was the Target of rapamycin complex subunit LST8 (from residues 8 to 324; Chain C) with a resolution of 3.5 Å.26 These two crystal structures were selected to build the final protein complex that has both the sites in one structure. As both structures have one common chain, hence would help in obtaining the complex.

Molecular Docking

Protein preparation

The PDB then was prepared using the Protein Preparation Wizard of Schrodinger Suite. Typical PDB structures normally only contain heavy atoms, waters, cofactors and metal ions, possibly unaligned terminal amide groups, and unassigned tautomeric and ionization states. Hence, PDB was pre-processed by assigning the correct bond orders, adding missing hydrogens, adding disulphide bong and converting selenomethionines to methionines. Protein was refined by optimizing sampling water orientations and hydrogen bonds. The minimization was performed using the OPLS3 force field with a maximum RMSD of 0.3 Å allowed to converge heavy atoms.

Ligand Preparation

The minimised protein contains two active sites (allosteric and kinase binding sites). The kinase site contains Adenosine Tri-Phosphate (ATP) as a co-crystallised ligand which can be prepared through LigPrep Module. The LigPrep module uses the OPLS3 force field for geometrical optimization. The LigPrep was used to generate the low-energy tautomeric, ionization and stereo-isomeric states at physiological pH 7.0_+2.0. The allosteric site has Rapamycin as a co-crystallised ligand attached to the protein. It is a macrocyclic compound that was prepared using Macrocycle sampling present in the conformation analysis of the Structural Analysis Module. Rapalink-1 is a third-generation ligand which is having allosteric binding part and a kinase binding part linked via a linker, was prepared manually by assigning the bond order, adding hydrogens, aligning the bond length, bond angle and inverting the chirality. Conformers were generated using the conformation search panel, including bioactive search in General modelling present in Maestro.

Pharmacophore Mapping

Hypothesis Generation

Ligand-Protein complex-based Pharmacophore Modelling is usually done by extracting common chemical features from a set of known ligand-protein complexes. The Pharmacophore Hypothesis and Scoring Engine (PHASE) module of Schrödinger software was employed to generate the Pharmacophoric hypothesis for Rapamycin complexed with the mTOR protein taken as a complex of ligand-protein. Similarly, a docked complex of ligand-protein at the active site having MLN-128 was taken for the Pharmacophore generation.

Built-in six Pharmacophoric features include hydrogen bond-acceptor (A), hydrogen bond-donor (D), hydrophobic group (H), negatively charged group (N), positively charged group (P), aromatic ring (R) is present in the PHASE Module, were used to define the chemical features of ligand that may help in finding out non-covalent bonding between the ligand and its target receptor. Scoring was done using Phase scorer and excluded volume shell was created from the ligand-protein complex space. The hypothesis performance is assessed by a small-scale virtual screening using the known actives and 1000 compounds Glide decoy set. Larger values of phase score indicate the hypothesis is more likely to perform well in virtual screening. PHASE looks for Pharmacophoric features that are common to all actives, but the condition is relaxed to 50 per cent.

RESULT AND DISCUSSION

Alignment of proteins

The alignment of both the PBD IDs (4DRI and 4JSV) has been performed using PyMOL.27 The RMSD value obtained after the alignment was 0.53 Å. Visualization of the aligned structure showed that Chain-B of 4DRI and Chain-A of 4JSV were aligning perfectly. Furthermore, the pairwise alignment using EMBOSS Needle of chain-A of 4JSV and Chain-B of 4DRI has been done to find out the similar residues in both protein sequences.[28] The results are shown below which further confirm that these are identical chains and therefore, can be used to build the final protein structure containing both sites.

Protein-Protein docking was also performed using Z-dock29 with the Chain-A of 4DRI containing rapamycin as a bound ligand and Chain-A of 4JSV. Results showed that the Chain-A of 4DRI containing rapamycin as a bound ligand dock with the chain-A of 4JSV at the identical residues which were present in the chain-B of 4DRI. The structure obtained after alignment was then saved as a new PDB.

Validation of docking protocol

The co-crystallized ligands present in the protein, Rapamycin and ATP, were obtained. Rapamycin was prepared through Macrocycle sampling and re-docked into the mTOR site which is an allosteric site. Similarly, ATP was prepared using Ligprep and re-docked into the mTOR kinase site. It was identified that both the co-crystallized ligands (Rapamycin and ATP) were almost superimposing to the native co-crystal ligands. The Root Mean Square Deviation (RMSD) of native and re-dock conformers of Rapamycin and ATP were in the range of 2.24 Å and 0.95 Å, respectively. Hence, validation of the reliability of docking calculations can be performed.

```
SEQUENCE   601 LIVASKSTITARHNAANKILKNMCEHSNTLVQQAMMVSEELIRVAILWHE   650
                                          ..|..|        :.|
SEQUENCE     1 ----------------------------------GAMDPE--------FME     9

SEQUENCE   651 MWHEGLEEASRLYFGERNVKGMFEVLEPLHAMMERGPQTLKETSFNQAYG   700
                 ||||||||||||||||||||||||||||||||||||||||||||||||||
SEQUENCE    10 MWHEGLEEASRLYFGERNVKGMFEVLEPLHAMMERGPQTLKETSFNQAYG    59

SEQUENCE   701 RDLMEAQEWCRKYMKSGNVKDLTQAWDLYYHVFRRISKQLPQLTSLELQY   750
                 ||||||||||||||||||||||||||||||||||||||||
SEQUENCE    60 RDLMEAQEWCRKYMKSGNVKDLTQAWDLYYHVFRRISKQ-----------    98

SEQUENCE   751 VSPKLLMCRDLELAVPGTYDPNQPIIRIQSIAPSLQVITSKQRPRKLTLM   800

SEQUENCE    99 --------------------------------------------------    98
```

Figure 3. Sequence alignment of 4DRI and 4JSV showing identical residues

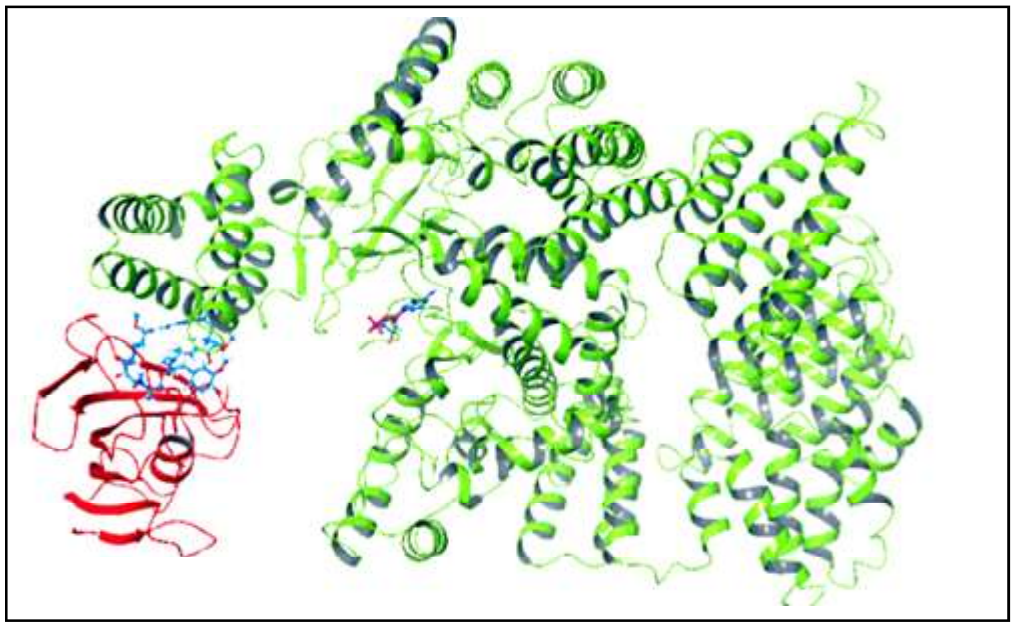

Figure 4. Structure of mTOR protein containing both allosteric site and active site formed after protein-protein docking.

Generation of Pharmacophore Models

The pharmacophore model for the active and allosteric sites was generated using the Phase module of Schrodinger software. For the Allosteric site, seven different features were found with two Acceptor groups (A9, A10), two Donor groups (D14, D15) and three hydrophobic groups (H23, H24, and H26). The geometry of the Allosteric site ligand (Rapamycin) AADDHHH is shown in figure 7(A) with their energy contributions. These

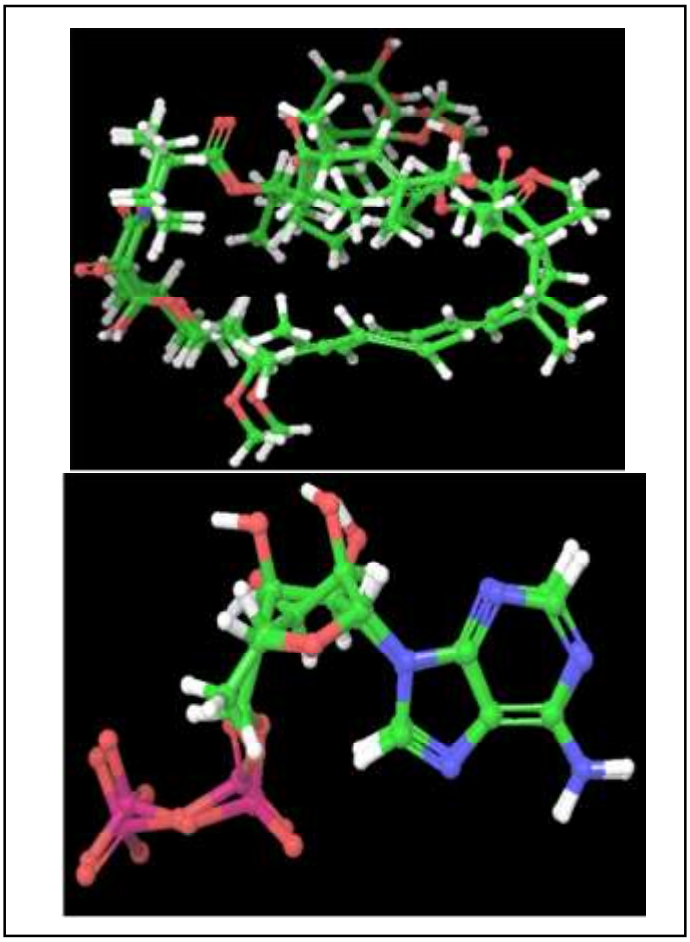

Figure 5. Superimposition of co-crystalized ligands (before and after redocking). a) Rapamycin b) ATP

features are based on the similarity of residues and ligands forming unique interactions. Acceptor groups such as A9 and A10 can accept hydrogen bonding from Ile87 and Tyr113 residues present nearby to the features. Similarly, donor feature D14 and D15 have Tyr57 and Gln85 in their neighbouring positions. Moreover, there are multiple hydrophobic residues around all three hydrophobic features (H23, H24, and H26) including Phe77, Val86, Trp90, Phe130, Phe2039, Trp2101, Tyr2105, and Phe2108. These features accommodate residues from both the chains forming the allosteric cavity, hence are important for binding.

The active site present on the mTOR protein generated four different features with the MLN0128 molecule. The common Pharmacophoric features include one Donor group (D7), one Hydrophobic group (H10) and two aromatic groups (R13 and R14). The geometry formed at the active site DHRR is shown in Figure 7(B). Donor group D7 is taken into consideration due to its interactions with Val2240. The two aromatic features (R13 and R14) have been considered as R13 fills up the space in the cavity and interacts with hydrophilic residues. The R14 group add planarity to the molecule and show pi-pi interaction with Trp2239 residue. Hydrophobic group H10 is exposed outside the cavity and therefore, would help add linker group.

Screening of Hit Molecules

The Pharmacophore models for common features were obtained for the allosteric as well as kinase binding sites based on Rapamycin and MLN-0128 as complexed ligands with the protein. Based on this, DrugBank and specs databases were employed for screening molecules after being prepared through Ligprep module of Schrodinger's software tool to obtain potential hits for the mTOR protein. The databases are selected based on already approved molecules as well as the commercial availability of molecules. Among this, 182 hits were obtained from the screening of DrugBank for the allosteric site and 682 for the kinase binding site. Also, about 14,797 and 84871 hits were obtained from the Specs

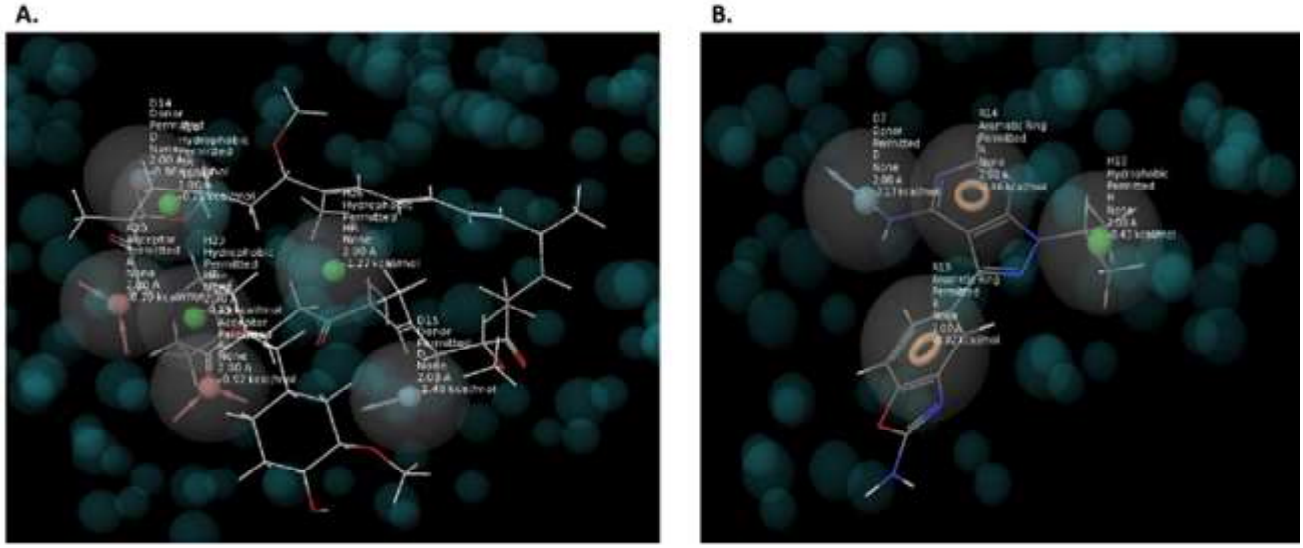

Figure 6. Pharmacophore map of (A)Rapamycin (for the allosteric site) and (B)MLN-0128 (Kinase site inhibitor) with common pharmacophoric features and their contribution

Table 2. Top 5 molecules screened after pharmacophore map for the allosteric site from DrugBank and Specs databases

SN.	Screened Drug Bank molecules at the allosteric site	Screened Specs molecules at the allosteric site
1.	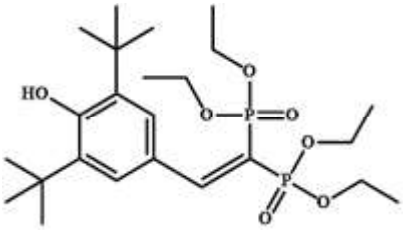 DB-AL-1 Fitness score-0.585	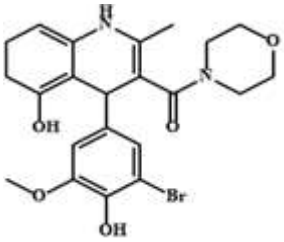 SP-AL-1 Fitness score-0.716
2.	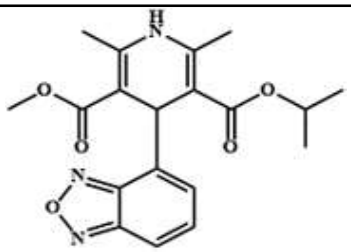 DB-AL-2 Fitness score-0.527	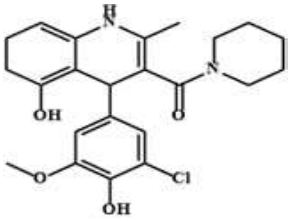 SP-AL-2 Fitness score-0.706
3.	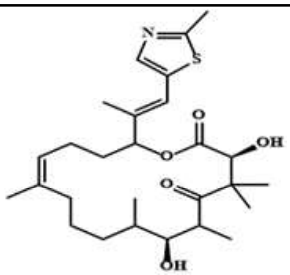 DB-AL-3 Fitness score-0.511	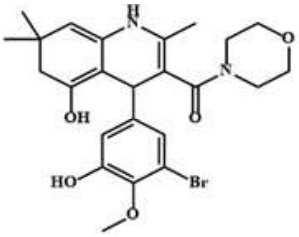 SP-AL-3 Fitness score-0.702
4.	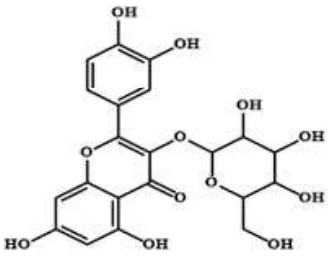 DB-AL-4 Fitness score-0.498	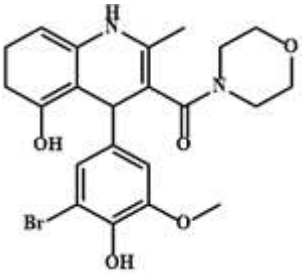 SP-AL-4 Fitness score-0.701
	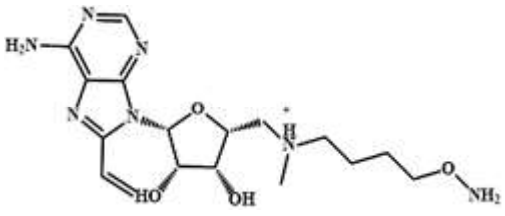 DB-AL-5 Fitness score-0.497	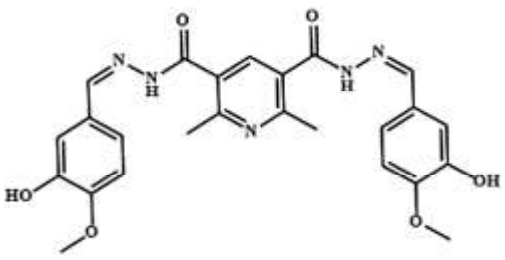 SP-AL-5 Fitness score-0.698

Table 3. Top 5 molecules screened after pharmacophore map for the Kinase site from DrugBank and Specs databases

SN.	Screened Drug Bank molecules at the kinase site	Screened Specs molecules at the kinase site
1.	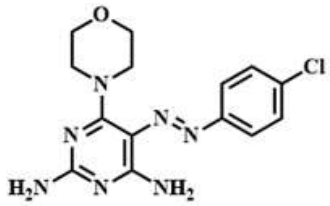 DB-KI-1 Fitness score-2.654	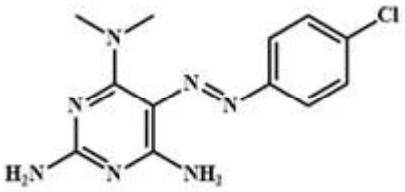 SP-KI-1 Fitness score-2.422
2.	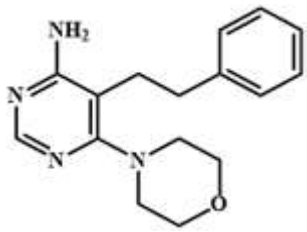 DB-KI-2 Fitness Score-2.654	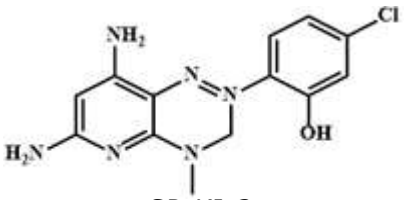 SP-KI-2 Fitness score-2.388
3.	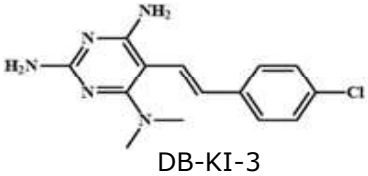 DB-KI-3 Fitness score-2.647	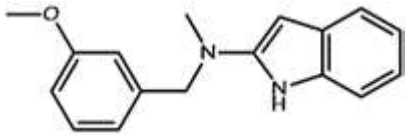 SP-KI-3 Fitness score-2.379
4.	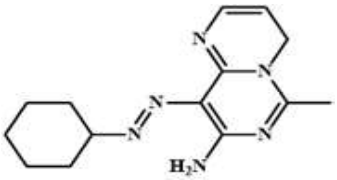 DB-KI-4 Fitness score-2.595	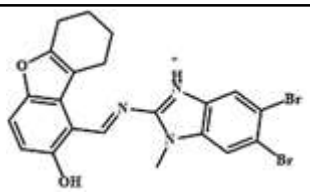 SP-KI-4 Fitness score-2.372
	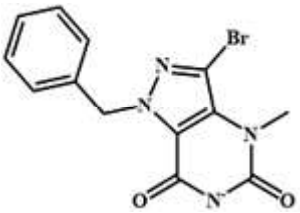 DB-KI-5 Fitness score-2.587	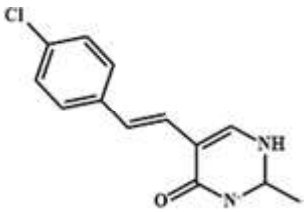 SP-KI-5 Fitness score-2.31

database for allosteric and kinase binding sites respectively. The top 5 hits, based on their fitness score among both databases have been shown in tabular form in Table.

Docking of screened molecules

The top 5 molecules based on fitness score for each site (Allosteric site and Kinase site) were obtained after the pharmacophore screening and were subjected to docking in their respective site on the complex protein. The docked hits were then analyzed based on their different scoring parameters, 3D conformations and interacting residues. The top scoring molecules i.e., DB-AL-4 (Docking score = -8.075 kcal/mol, glide emodel = -73.005 kcal/mol) from Drugbank and SP_AL-5 (docking score = -7.239 kcal/mol, glide emodel = -83.930 kcal/mol) from Specs database were having more relevant poses. These two molecules have more interactions and have more native-like binding poses. Molecule DB-

Table 4. Details of top 10 hits obtained after docking at the allosteric site of mTOR protein complex

S.N	Molecule	Interacting residues	Docking score	Glide Emodel
1.	DB_AL_4	Hbond-Arg73, Val78, Gln85, Ser2035, Asp2102; π-π interactions-Phe2039, Trp2101; Hydrophobic- Phe77, Phe2039, Trp2101, Tyr2105, Phe2108	-8.075	-73.005
2.	SP_AL_5	Hbond- Arg73, Tyr113, Leu119; π-π interactions-Trp2101; Hydrophobic- Phe77, Lys121, Ile122, Phe2039, Trp2101, Tyr2105	-7.239	-83.930
3.	DB_AL_5	Hbond- Asp2102, Arg2036; π-cation-Phe2039, Tyr2105; Hydrophobic interactions- Phe2039, Trp2101, Tyr2105, Phe2108	-7.767	-81.882
4.	SP_AL_4	Hbond- Tyr57; Hydrophobic- Phe77, Val86, Ile87, Trp90, Phe2039, Trp2101, Tyr2105	-6.666	-59.994
5.	SP_AL_2	Hbond- Tyr57; Hydrophobic- Phe77, Val86, Ile87, Trp90, Phe2039	-6.666	-59.994
6.	DB_AL_2	Hbond- Ile87; π-cation- Arg73; Hydrophobic- Phe67, Asp68, Phe77, Phe2039, Trp2101, Tyr2105	-6.402	-57.674
7.	SP_AL_3	Hbond- Tyr57; Hydrophobic- Phe67, Asp68, Phe77, Phe2039	-6.027	-59.890
8.	DB_AL_3	Hydrophobic-Phe77, Ile87, Phe2039, Trp2101, Tyr2105	-5.840	-52.455
9.	SP_AL_1	Hbond-Ser118; Hydrophobic- Phe77, Val86, Ile87, Trp90, Phe2039, Trp2101	-5.798	-65.132
10.	DB_AL_1	Hbond-Tyr113, Ser118; π-π interactions-Phe77; Hydrophobic- Phe77, Val86, Ile87, Trp90, Phe130, Phe167 Phe2039, Trp2101, Tyr2105	-5.733	-56.115

AL-4 retains some of the native hydrogen bonds (Gln85) and hydrophobic interactions (Phe2039, Trp2101, Tyr2105, Phe2108) while also introduces new hydrogen bonding (Ser2035, Asp2102) and p-p staking interactions (Phe2039, Trp2101). Similarly, SP_AL-5 retained native interactions such as hydrogen bonds with Arg73, Gln85 and Hydrophobic interactions with Phe2039, Trp2101, Tyr2105, and Phe2108. However, it also formed hydrogen bonds with Val78, Ser2035, Asp2102 and p-p interactions with Phe2039, Trp2101. Moreover, these interactions were aligning with the pharmacophoric features of allosteric site. More details for all the docking results of molecules for the allosteric site are added in Table 4.

Top scoring molecules i.e., DB-KI-2 (docking score = -8.218 kcal/mol, glide emodel = -57.903 kcal/mol) and DB-KI-1 (docking score = -8.121 kcal/mol, glide emodel = -60.460 kcal/mol) from Drugbank were selected as kinase site binding ligands. DB-KI-2 have similar interactions as the native inhibitor MLN-0128 such as hydrogen bond with Asp2195, Tyr2225; p-p interactions with Trp2239 and hydrophobic interactions with Leu2185, Ileu2237, Trp2239, Met2345. This molecule makes added some new interactions such as a hydrogen bond with Asp2357 and hydrophobic interactions with Cys2243. Similar to this, DB-KI-1 was also a good hit generated through kinase site pharmacophore. This molecule had native interactions such as hydrogen interactions with Asp2195, Tyr2225; p-p interactions with Trp2239 and hydrophobic interactions with

Table 5. Details of top 10 hits obtained after docking at the kinase site of mTOR protein complex

S.N	Molecule	Interacting residues	Docking score	Glide Emodel
1.	DB_KI_2	Hbond-Asp2195, Tyr2225, Val2240, Asp2357; π-π interactions-Trp2239; Hydrophobic-Leu2185, Ile2237, Trp2239, Cys2243, Met2345	-8.218	-57.903
2.	SP_KI_2	Hbond-Asp2195, Tyr2225, Asp2357; π-π interactions-Trp2239; Hydrophobic-Leu2185, Ile2237, Trp2239, Met2345	-8.128	-57.703
3.	DB_KI_1	Hbond-Asp2195, Tyr2225, Asp2357; π-π interactions-Trp2239; Halogen bond-Cys2243 Hydrophobic-Leu2185, Ile2237, Trp2239, Cys2243, Met2345, Ile2356	-8.121	-60.460
4.	DB_KI_4	Hbond-Val2240; Hydrophobic- Trp2239, Asp2244, Thr2245, Met2345	-7.836	-54.524
5.	SP_KI_1	Hbond-Val2240; Hydrophobic- Trp2239, Asp2244, Thr2245, Met2345	-7.836	-60.525
6.	DB_KI_3	Hbond- Cys2243; π-π interactions- Trp2239; Halogen bond-Ser2342; Hydrophobic-Leu2185, Ile2237, Trp2239, Cys2243, Thr2245, His2247, Ala2248, Met2345, Ile2356	-7.632	-63.126
7.	SP_KI_4	Hbond-Val2240; Hydrophobic-Leu2185, Ile2237, Trp2239, Cys2243, Ala2248, Met2345, Ile2356	-7.426	-60.828
8.	DB_KI_5	Salt Bridge- Lys2187; Hydrophobic-Tyr2225, Trp2239, Thr2245, Met2345, Leu2354, Ile2356	-6.922	-52.887
9.	SP_KI_5	Hbond-Val2240; π-π interactions-Trp2239; Hydrophobic-Lys2187, Leu2185, Ile2237, Trp2239, Ile2356, Aps2357	-6.220	-57.765
10.	SP_KI_3	Hbond- Val2240, Cys2243 ?-? interactions-Trp2239; Hydrophobic-Lys2187, Leu2192, Leu2185, Ile2237, Ile2356	-3.791	-40.735

Leu2185, Ileu2237, Trp2239, Met2345, Leu2356. There were newly formed hydrogen interactions with Asp2257; hydrophobic interactions with Cys2243 and Halogen bonded interactions with Cys2243. Molecule SP_KI_2 has a higher score as can be inferred from Table 5, however, it formed lesser interactions with protein residues at the kinase site and have higher clashes with less glide emodel score. Finally, these top-scoring molecules with more relevant poses at the sites were selected for the design of third-generation molecules as mTOR inhibitors.

Design of third-generation mTOR inhibitors

The design aspect of third-generation mTOR inhibitors utilized both ligands together, tethered via a linker between them. The top two molecules from each site were selected from the docked ligands from each site as they have high-scoring and more refined poses than other ligands. Most common linker molecules such as Alkyl, PEG were utilized to provide enough distance that accommodates stable interactions for both sites and keep both ligands bound within their binding site. The linker attachment was assessed by finding out the water-exposed part of each ligand at the allosteric site and kinase site. After analyzing the total distance between the two sites, around 25Å was required to join the linkers with the exposed group at both ends. Both Alkyl and PEG with suitable lengths were selected for the design of Alkyl-based and PEG based molecules and a total of four designed molecules were obtained in the end.

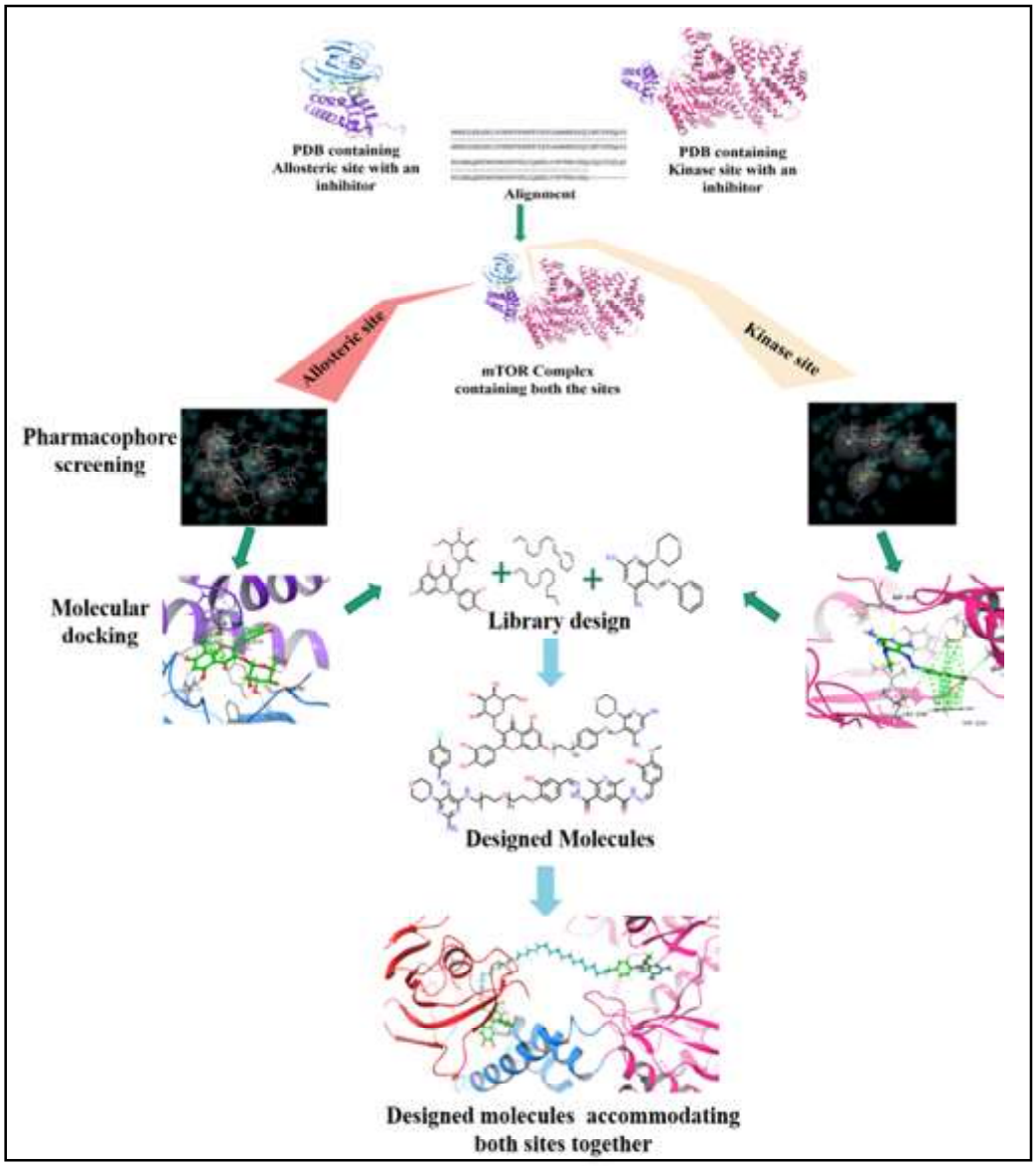

Figure 7. Overview of the computational workflow applied in designing next-generation mTOR inhibitors

Finally, these designed molecules were docked to the protein after being prepared. Designed molecules with alkyl linkers have shown less conformational changes and were able to accommodate both the site. While PEG-based linkers show more flexibility and interact with other residues to form closed conformations and were not able to bind both site at once. The coverage of alkyl-based linked molecules was more in the binding site; therefore, alkyl-based linkers were more relevant in the study. These alkyl linkers also make suitable interactions with tunned residues and offer more stability to the molecule. One of the molecules, DB_AL_4_Alkyl_DB_KI_2 (Molecule 1) shows identical binding poses as their individual ligands and hence, is considered. Kinase site interactions such as hydrogen bonds with Val2240 and hydrophobic interactions with Trp2239 residues were still present with other interactions. Parallel to this, allosteric site interactions were also present including hydrogen bonding with hydrophobic interactions with Phe77, Trp2101, Tyr2105, and Phe2039. Molecule 1 aligned more significantly over the individual ligands and retains similar interactions in the binding site. Moreover, the alkyl linker also interacted with tunnel residues such as Ile49, Ile87, Lys88, and Lys2166 through hydrophobic contacts, offering it more stability within the space.

CONCLUSION

mTOR is one of the attractive and explored targets against therapeutic conditions such as in cancer therapy including advanced renal cell carcinoma, pancreatic neuroendocrine tumours, advanced breast cancer, arthritis, insulin resistance, osteoporosis, and other diseases. The role of mTOR in cancer metabolism has significance, however, it remains challenging to target the protein due to clinical limitations, mutations, resistance, negative feedback loop and stronger toxicity. Although, there are approaches that are being applied to inhibit the apparent activity of the protein. Next-generation mTOR inhibitors have excited researchers and mounded into a new path. In this study, the design of new molecules that bind both sites of mTOR i.e.; kinase site and allosteric site is reporting through rational design using computational approaches. A complex of protein containing both the site is prepared which can be evident for screening of molecules on both sites. This also helped in rationalising the distance between the two cavities and integrating appropriate linkers between the two ligands. Moreover, Pharmacophore map and docking analysis supported filtering stronger affinity ligands at the sites. Finally,

Table 6. Designed next-generation mTOR inhibitors with alkyl and PEG linkers added to the table with their 2D structure and scoring parameters

S.N	Designed Molecules	2D structure of designed molecules	Docking score	Glide Emodel
1.	DB_AL_4_Alkyl_DB_KI_2 (Moleccule1) (alkyl based)	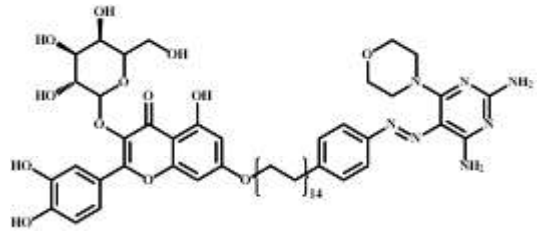	-13.725	-168.122
2.	SP_AL_5_Alkyl_DB_KI_1 (Moleccule2) (alkyl based)	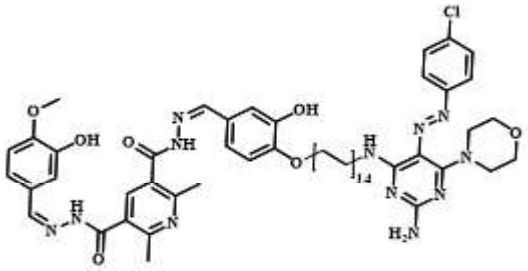	-8.525	-102.392
3.	DB_AL_4_PEG_DB_KI_2 (Moleccule3) (PEG-based)	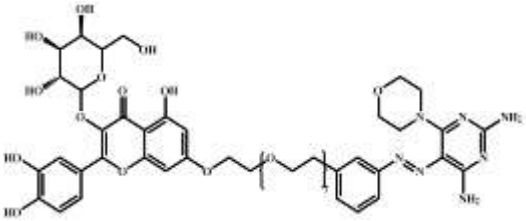	-7.346	-115.661
4.	SP_AL_5_PEG_DB_KI_1 (Moleccule4) (PEG-based)	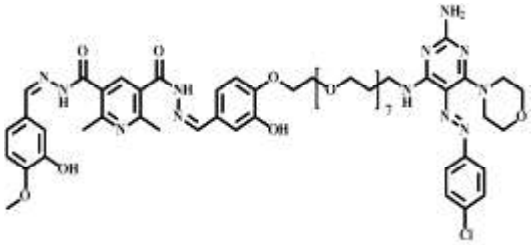	-10.558	-168.762

after vigorous and computationally expensive investigation, the alkyl linker-based molecules have shown important interactions with both sites and blocked them, simultaneously. Overall, this study would serve as a design strategy for next-generation mTOR inhibitors. These results can be extrapolated in the in-vitro and in-vivo study for validation and clinical applications of this new class of inhibitors.

References

1. Aktipis, C. A., Boddy, A. M., Jansen, G., Hibner, U., Hochberg, M. E., Maley, C. C., Wilkinson, G. S. (2015) Cancer across the tree of life: cooperation and cheating in multicellularity. Philos. Trans. R. Soc. B: Biol. Sci, 370, 1673
2. Fadaka, A., Ajiboye, B., Ojo, O., Adewale, O., Olayide, I., Emuowhochere, R. (2017). Biology of glucose metabolization in cancer cells. J. Oncol, 3, 45-51
3. Schcolnik-Cabrera, A., Chávez-Blanco, A., Domínguez-Gómez, G., Dueñas-González, A. (2017). Understanding tumor anabolism and patient catabolism in cancer-associated cachexia. Am. J. Cancer Res, 7, 1107-1115
4. DeBerardinis, R. J., Chandel, N. S. (2016). Fundamentals of cancer metabolism. Sci. Adv, 2, 15-19
5. Martinez-Outschoorn, U. E., Peiris-Pagés, M., Pestell, R. G., Sotgia, F., Lisanti, M. P. (2017). Cancer metabolism: a therapeutic perspective. Nat Rev Clin Oncol, 14, 11-31
6. Claude, A. (1949). Proteins, Lipids, and Nucleic Acids in, Cell Structures and Functions. Adv Protein Chem , 5, 423-440

7. Sabatini, D. M. (2017). Twenty-five years of mTOR: Uncovering the link from nutrients to growth. Proc. Natl. Acad. Sci. , 114, 11818-11825
8. Huang, S., Houghton, P. J. (2003). Targeting mTOR signaling for cancer therapy. Curr Opin Pharmacol, 3, 371-377
9. Sancak, Y., Peterson, T. R., Shaul, Y. D., Lindquist, R. A., Thoreen, C. C., Bar-Peled, L., Sabatini, D. M. (2008). The Rag GTPases bind raptor and mediate amino acid signaling to mTORC1. Science, 320, 1496-1501
10. Guertin, D. A., Sabatini, D. M. (2009). The pharmacology of mTOR inhibition. Sci Signal, 2, 67-78
11. Kim, S. G., Buel, G. R., Blenis, J. (2013). Nutrient regulation of the mTOR complex 1 signaling pathway. Mol. Cells, 35, 463-473
12. Suryawan, A., Davis, T. A. (2018). Amino acid- and insulin-induced activation of mTORC1 in neonatal piglet skeletal muscle involves sestrin2-GATOR2, Rag A/C-mTOR, and RHEB-mTOR complex formation. J. Nutr, 148, 825-833
13. Jia, J., Abudu, Y. P., Claude-Taupin, A., Gu, Y., Kumar, S., Choi, S. W., Deretic, V. (2019). Galectins control MTOR and AMPK in response to lysosomal damage to induce autophagy. Autophagy, 15, 169-171
14. Burris, H. A. (2013). Overcoming acquired resistance to anticancer therapy: focus on the PI3K/AKT/mTOR pathway. Cancer Chemother. Pharmacol, 71, 829-842
15. Levy, D. S., Kahana, J. A., Kumar, R. (2009). AKT inhibitor, GSK690693, induces growth inhibition and apoptosis in acute lymphoblastic leukemia cell lines. Blood, 113, 1723-1729
16. Seto, B. (2012). Rapamycin and mTOR: a serendipitous discovery and implications for breast cancer. CLIN TRANSL MED, 1, 1-7
17. Arriola Apelo, S. I., Lamming, D. W. (2016). Rapamycin: an InhibiTOR of aging emerges from the soil of Easter Island. J. Gerontol, 71, 841-849
18. Zhang, Y. J., Duan, Y., Zheng, X. S. (2011). Targeting the mTOR kinase domain: the second generation of mTOR inhibitors. Drug Discov. Today, 16, 325-331
19. Rodrik-Outmezguine, V. S., Okaniwa, M., Yao, Z., Novotny, C. J., McWhirter, C., Banaji, A., Shokat, K. M. (2016). Overcoming mTOR resistance mutations with a new-generation mTOR inhibitor. Nature, 534, 272-276
20. Chresta, C. M., Davies, B. R., Hickson, I., Harding, T., Cosulich, S., Critchlow, S. E., Pass, M. (2010). AZD8055 is a potent, selective, and orally bioavailable ATP-competitive mammalian target of rapamycin kinase inhibitor with in vitro and in vivo antitumor activity. Cancer Res., 70, 288-298.
21. Chen, Y., Zhou, X. (2020). Research progress of mTOR inhibitors. Eur. J. Med. Chem, 208, 112-118
22. Martins, F., de Oliveira, M. A., Wang, Q., Sonis, S., Gallottini, M., George, S., Treister, N. (2013). A review of oral toxicity associated with mTOR inhibitor therapy in cancer patients. Oral Oncol., 49, 293-298
23. Xu, T., Sun, D., Chen, Y. Ouyang, L. (2020) Targeting mTOR for fighting diseases: A revisited review of mTOR inhibitors. Eur. J. Med. Chem , 199, 112-119
24. März, A. M., Fabian, A. K., Kozany, C., Bracher, A., Hausch, F. (2013). Large FK506-binding proteins shape the pharmacology of rapamycin. Mol. Cell. Biol, 33, 1357-1367
25. Yang, H., Rudge, D. G., Koos, J. D., Vaidialingam, B., Yang, H. J., Pavletich, N. P. (2013). mTOR kinase structure, mechanism and regulation. Nature, 497, 217-223
26. Ouvry, G., Clary, L., Tomas, L., Aurelly, M., Bonnary, L., Borde, E., Hennequin, L. F. (2019). Impact of minor structural modifications on properties of a series of mTOR inhibitors. ACS Medicinal Chem. Lett, 10, 1561-1567
27. DeLano, W. L. (2002). Pymol: An open-source molecular graphics tool. Protein Crystallogr., 40, 82-92
28. Needleman, S. B., Wunsch, C. D. (1970). A general method applicable to the search for similarities in the amino acid sequence of two proteins. J. Mol. Biol, 48, 443-453
29. Pierce, B. G., Hourai, Y., Weng, Z. (2011). Accelerating protein docking in ZDOCK using an advanced 3D convolution library. PloS One, 6, 246-257